Unique charge distribution in surface loops confers high velocity on the fast motor protein *Chara* myosin

Kohji Ito[1], Yukie Yamaguchi, Kenji Yanase, Yousuke Ichikawa, and Keiichi Yamamoto

Department of Biology, Chiba University, Inage-ku, Chiba City, Chiba 263-8522, Japan

Edited by James A. Spudich, Stanford University, Stanford, CA, and approved October 26, 2009 (received for review September 18, 2009)

Most myosins have a positively charged loop 2 with a cluster of lysine residues that bind to the negatively charged N-terminal segment of actin. However, the net charge of loop 2 of very fast *Chara* myosin is zero and there is no lysine cluster in it. In contrast, *Chara* myosin has a highly positively charged loop 3. To elucidate the role of these unique surface loops of *Chara* myosin in its high velocity and high actin-activated ATPase activity, we have undertaken mutational analysis using recombinant *Chara* myosin motor domain. It was found that net positive charge in loop 3 affected V_{max} and K_{app} of actin activated ATPase activity, while it affected the velocity only slightly. The net positive charge in loop 2 affected K_{app} and the velocity, although it did not affect V_{max}. Our results suggested that *Chara* myosin has evolved to have highly positively charged loop 3 for its high ATPase activity and have less positively charged loop 2 for its high velocity. Since high positive charge in loop 3 and low positive charge in loop 2 seem to be one of the reasons for *Chara* myosin's high velocity, we manipulated charge contents in loops 2 and 3 of *Dictyostelium* myosin (class II). Removing positive charge from loop 2 and adding positive charge to loop 3 of *Dictyostelium* myosin made its velocity higher than that of the wild type, suggesting that the charge strategy in loops 2 and 3 is widely applicable.

actin | ATPase | motility | cytoplasmic streaming | molecular engineering

Cytoplasmic streaming in characean algal cells is extremely fast, and this streaming is brought about by the movement of myosin-coated organelles along actin filament bundles fixed inside the cell (1). Myosin purified from *Chara corallina* could translocate actin filaments in the in vitro motility assay at a velocity comparable to that of the cytoplasmic streaming (approximately 50 $\mu m\ s^{-1}$) (2, 3). This velocity is about 10 times faster than that of the fast skeletal muscle myosin and the *Chara* myosin is the fastest motor protein known so far. We have cloned cDNA of the *Chara* myosin heavy chain (4) and succeeded in expressing functional motor domain (5, 6). The velocity of the expressed motor domain measured by in vitro motility assay was comparable to that of the native *Chara* myosin if we consider the difference in the lever arm length. Relevant steps in actomyosin ATPase cycle to the sliding velocity are ADP release from actomyosin and ATP reassociation resulting in actin-myosin dissociation. Kinetic analyses of *Chara* myosin motor domain revealed that both the ADP release and the ATP-induced dissociation from actin were very fast (6). Time spent in the strongly bound state with actin, which was estimated from these rates, was less than 1 ms. This very short strongly bound state, together with a large step size (7), are probably the reason for the very high velocity of *Chara* myosin. Actin-activated ATPase activity of expressed *Chara* motor domain was approximately 500 $s^{-1}head^{-1}$, which was also the highest of all myosins so far measured (5). Since the ADP release and ATP-induced dissociation was very fast as mentioned above, the rate-limiting step of acto-*Chara* myosin ATPase is suggested to be the transition from the weekly to the strongly bound state with actin with concomitant release of Pi (6).

It is known that mutations in various surface loops that interact with actin affect these steps (8). In this study, we focused our attention on loops 2 and 3 of *Chara* myosin. Loops 2 and 3 are part of actin binding sites (9, 10). Cross-linking studies suggested that positively charged residues in loops 2 and 3 interact with negatively charged residues in subdomain 1 of actin at the initial weakly bound state (11–21).

Since these surface loops are highly variable in sequence and length among various classes of myosins (Tables 1 and 2), it is suggested that diverse enzymatic and motile activities of the myosins are achieved in part through the variations in the sequences of these loops (22, 23). Many studies have revealed the relationship between positive charge of loop 2 and actin-activated ATPase activities (24–29).

Chara myosin has unique feature in these surface loops: the net charge of loop 2 is zero and that of loop 3 is the largest among all myosins so far known (Tables 1 and 2). To elucidate the role of these unique surface loops of *Chara* myosin in its high velocity and high actin-activated ATPase activity, we studied the activity of recombinant *Chara* myosin motor domains in which charge and length of these loops were altered. We found that the actin-activated ATPase activity of *Chara* myosin was highly dependent on the net positive charge in loop 3 while the velocity was not. We also found that addition of positive charge to loop 2 had only small effect on the actin-activated ATPase activity but greatly reduced the ADP release rate and thus the velocity of *Chara* myosin.

Results

Expression and Purification of Mutants. Because recombinant *Chara* myosin motor domains used in this study contain only motor domain but not IQ motifs while native *Chara* myosin has 6 IQ motifs, lever arm length, and thus the velocity of the recombinant *Chara* myosin motor domains, are about one-eighth of those of the native *Chara* myosin (5, 6). Loops 2 and 3 of the motor domain were mutated by PCR-based mutagenesis. After expression in insect cells, mutant motor domains were purified by coprecipitation with actin and by nickel-affinity resin. However, we could not use the coprecipitation with actin for mutant motor domains whose affinity for actin was very low. These mutant motor domains were further fused with FLAG tag and purified by Ni-affinity resin and anti-FLAG antibody resin.

Loop 3 Mutants. *Chara* myosin has very short loop 2 with no net charge (Table 1), but its apparent affinity for actin in the presence of ATP (estimated from K_{app} of actin-activated ATPase activity) was much higher than that of skeletal muscle myosin that has a long and positively charged loop 2 (Table 1 and Fig. 1). *Chara* myosin, on the other hand, has much more positive net charge in loop 3 than any other myosins (Table 2). Since this loop of skeletal (11) and cardiac muscle (21) myosins is also cross-linked to actin, we first altered net charge in loop 3 systemically by substituting positively charged amino acids to alanine or by adding lysine residues and examined the effect on the functional characteristics of *Chara* myosin.

Author contributions: K.I. and K. Yamamoto designed research; K.I., Y.Y., K. Yanase, and Y.I. performed research; K.I. contributed new reagents/analytic tools; K.I., Y.Y., K. Yanase, and Y.I. analyzed data; and K.I. and K. Yamamoto wrote the paper.

The authors declare no conflict of interest.

This article is a PNAS Direct Submission.

[1]To whom correspondence should be addressed. E-mail: k-ito@faculty.chiba-u.jp.

Table 1. Loop 2 sequences of various myosins

Source*	Length	Net charge	Sequence†
Chara	17	0	FP A*DE*GT**K**APS**K**FMSIG
Chick Sk	28	+3	FATYG G*EA*E**G**GGG**KK**GG**KKK**GSSFQTVS
Chick Sm	36	+3	W**K***D***V***D***R**IV GL*D*QM A**K**MT*ES*SLPSAS**K**T**KK**GMF**R**TVG
Chick Va	45	+6	FQ*DEE***K**AISPTSATPSG**R**VPLS**R**TPV**K**PA**K**A**R**PGQTS**K***E***HKK**TVG

*_Chara_ (_Chara corallina_ myosin XI), Chick Sk (Chicken fast skeletal myosin II), Chick Sm (Chicken smooth muscle myosin II), Chick Va (Chicken myosin Va).
†Positively and negatively charged amino acids are shown in bold and italic, respectively.

We made 4 loop 3 mutant motor domains (Table 3). A mutant designated L3 (-5) has substitutions at all 5 positively charged amino acids of loop 3. L3 (N-3) has substitutions at 3 positively charged amino acids at the N-terminal side of loop 3. L3 (C-2) has substitutions at 2 positively charged amino acids at the C-terminal side of loop 3. L3 (+2) has 2 additional lysine residues at the N-terminal side of loop 3.

Fig. 2 shows actin concentration dependence of the ATPase activities of loop 3 mutants. Data were fitted to the Michaelis-Menten equation and V_{max} and K_{app} values for each mutant were determined. Both V_{max} and K_{app} were affected by the net positive charge in loop 3 (Table 3). When net positive charge in loop 3 was reduced from + 5 to + 2 [L3 (N-3) mutant], V_{max} decreased to 45% and K_{app} increased (apparent affinity for actin decreased) from 23 μM to 81 μM. We could not determine both V_{max} and K_{app} of L3 (-5) mutant because the activity of L3 (-5) increased almost linearly with actin concentration (Fig. 2). Increase in the net positive charge in loop 3 by adding 2 lysine residues [L3 (+2)] lowered K_{app} but V_{max} also became lower than that of the wild type (Table 3), suggesting that there might be an optimal amount of positive charge and/or optimal length for loop 3. Actin cosedimentation assays using wild-type and L3 (-5) mutant also supported the effect of the positive charge of loop 3 on the actin affinity. Because *Chara* myosin has very high actin-activated ATPase activity and most ATP would be depleted during the standard actin cosedimentation assay, we used nonhydrolyzable ATP analog AMP-PNP in our cosedimentation assays. K_d (dissociation constant for actin) of wild type and L3 (-5) were 7.3 μM and 190 μM, respectively. These results showed that the affinity of *Chara* myosin for actin was largely dependent on the positive charge of loop 3.

In contrast to the ATPase activity, charge alteration of loop 3 did not affect the velocity so much. For example, V_{max} of L3(N-3) was only 45% that of the wild type but its velocity was 90% that of the wild type (Table 3). ATPase activity of L3(-5) was less than 10% that of the wild type at all actin concentrations measured (Fig. 2). Due to very low affinity for actin, L3(-5) could not move actin filaments in the standard buffer for in vitro motility assay. However, in the presence of 0.8% methylcellulose that prevent detachment of actin filaments from the myosin-coated surface (30), the velocity of L3(-5) could be observed, and it was 70% that of the wild type (Table 3).

Table 2. Loop 3 sequences of various myosins

Source*	Length	Net charge	Sequence†
Chara	6	+5	**KHKFKR**
Chick Sk	10	+3	**KPK**PA**K**G**K**A*E*
Chick Sm	8	+3	**KSK**QL**K**D**K**
Chick Va	6	+2	**KPR**LSN

*_Chara_ (_Chara corallina_ myosin XI), Chick Sk (Chicken fast skeletal myosin II), Chick Sm (Chicken smooth muscle myosin II), Chick Va (Chicken myosin Va).
†Positively and negatively charged amino acids are shown in bold and italic, respectively.

Loop 2 Mutants. Loop 2 of *Chara* myosin is very short and has only 2 positively charged amino acids. Unlike other myosins, these 2 lysine residues are not in a cluster but separated by 3 aa residues (Table 1). We designated a lysine residue at the N-terminal side as "lysine-N" and one at the C-terminal side as "lysine-C". To estimate the contribution of loop 2 to the actin-activated ATPase activity and velocity of *Chara* myosin, we made 7 loop 2 mutants (Table 4). L2 (-2) has substitutions to alanine at both lysine-N and lysine-C. L2 (N-1) and L2 (C-1) have substitution at the lysine-N and at the lysine-C, respectively. L2 (N+2) has additional GGKKGG sequence at the N-terminal side of lysine-N. Skeletal and smooth muscle myosins have 2 to 3 successive lysine residues near the C-terminal end of loop 2 (Table 1) and the importance of these lysine residues in the interaction with actin is reported (17, 31). Thus, we intended to generate such a lysine cluster in loop 2 by adding 2 lysine residues (KK) to the C-terminal side of lysine-C and designated this as L2 (C+2). L2 (+4) has GGKKGG at the N-terminal side of lysine-N and KK at the C-terminal side of lysine-C. This mutant has loop 2 that is very similar in charge composition and length to that of skeletal muscle myosin among mutants used in this study. We also made a mutant L2 (N+0) that has GGAAGG at the N-terminal side of lysine-N to see the effect of length change in loop 2 without charge alteration.

Unlike loop 3 mutants, net charge in loop 2 had only limited effect on V_{max} (Table 4). However, it dramatically affected the velocity with a concomitant change in K_{app} (Table 4). The velocity of L2 (C-1) and L2 (-2) increased by 20 to 30% with the increase in K_{app} (a decrease in the apparent affinity for actin), but those of L2 (N-1) were almost the same as those of the wild type (Table 4), suggesting large contribution of lysine-C to the interaction with actin. In contrast, the velocity of L2 (N+2) and L2 (C+2) dropped to 35 to 50% that of the wild type with the decrease in K_{app} (Table 4). Addition of 4 lysine residues to *Chara*

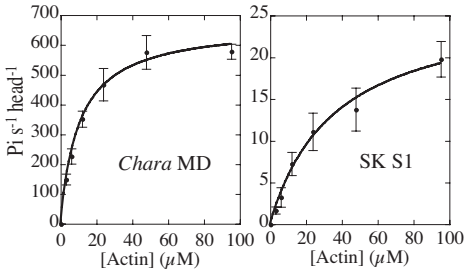

Fig. 1. Actin-activated ATPase activities of *Chara* myosin motor domain and skeletal myosin subfragment-1. Values are averages of 3 measurements. Data were fitted to the Michaelis-Menten equation. V_{max} of *Chara* myosin motor domain and skeletal myosin subfragment-1 (S1) were 670 ± 20 and 27 ± 2 Pi/s/head, respectively. K_{app} values of *Chara* myosin motor domain and skeletal myosin S1 were 11 ± 1 and 27 ± 2 μM, respectively. Note that the ATPase assays shown in this figure were done at low salt (10 mM KCl, 4 mM $MgCl_2$, 20 mM Hepes-KOH, pH 7.4) because the ATPase activity of skeletal myosin S1 in standard ATPase assay solution increased linearly with the increase in actin concentration and both V_{max} and K_{app} values could not be determined.

Table 3. Sequences, net charge and activity of wild type and loop 3 mutants of *Chara* myosin motor domain

	Sequence*	Net charge	V_{max} (Pi/head/s)†	K_{app} (μM)†	Velocity (μm/s)§
L3 (−5)	*AAAFAA*	0	ND‡	ND‡	3.3 ± 0.2¶
L3 (N-3)	*AAA*F**KR**	+2	260	81	4.3 ± 0.3
L3 (C-2)	**KHK**F*AA*	+3	540	44	4.5 ± 0.2
WT	**KHK**F**KR**	+5	580	23	4.8 ± 0.2
L3 (+2)	*KK***KHK**F**KR**	+7	390	12	4.3 ± 0.2

*Positively charged amino acid and altered amino acid are shown in bold and italic, respectively.
†Values are averages of two measurements on two independent preparations.
‡We could not determine V_{max} and K_{app} of L3 (−5) because activity increased almost linearly (see Fig. 2).
§Values are averages ± SD of 40–50 actin filaments on two independent preparations.
¶Velocity of L3 (−5) was done in the presence of 0.8% methylcellulose.

loop 2 [L2 (+4)], further lowered the velocity (23% that of the wild type, Table 4) with further decrease in K_{app}. Change in the length of loop 2 had little effect on the functional characteristics of *Chara* myosin [L2 (N+0) mutant, Table 4]. *Chara* myosin motor domain seems to have allowance for long loop 2.

Kinetics. Although charge alteration in loop 2 did not affect the V_{max} of the actin-activated ATPase activity so much, we observed obvious effect on the velocity. In particular, the velocity of L2 (+4) was considerably lower than that of the wild type as mentioned above. In general, velocity depends on the time of strongly bound state with actin, which is determined by ADP dissociation rate from acto-myosin·ADP complex and acto-myosin dissociation rate by ATP binding (32, 33). Thus, it is anticipated that the slow movement of L2 (+4) is due to reduction in either of these 2 rates or in both. So we measured the rates of mantADP release from acto-L2 (+4)·mantADP and ATP-induced dissociation of acto-L2 (+4) using stopped flow technique. As shown in Fig. 3*A*, mantADP release rate from acto-L2 (+4)·mantADP (480 ± 70 s^{-1}) was less than 20% that of the wild type (2800 s^{-1}) (6). In contrast, ATP-induced acto-L2 (+4) dissociation rate (4.0 μM^{-1} s^{-1}, Fig. 3*B*) was almost the same as that of the wild type (4.1 μM^{-1} s^{-1}) (6). These results suggest that low velocity of L2 (+4) is due to slow ADP release from acto-L2 (+4)·ADP.

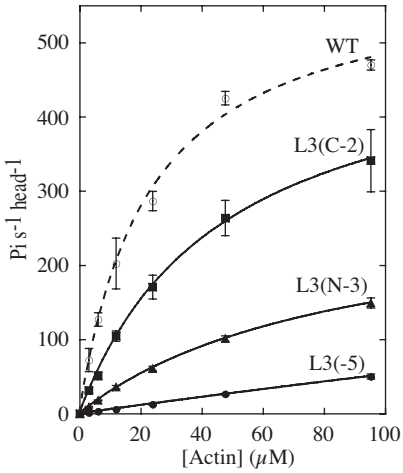

Fig. 2. Actin-activated ATPase activities of wild-type and loop 3 mutants of *Chara* myosin motor domain. Values are averages of 3 measurements for each mutant preparation. V_{max} and K_{app} were determined by fitting data to the Michaelis-Menten equation. Averaged V_{max} and K_{app} values from 2 independent preparations were shown in Table 3. Because the activity of L3 (-5) increased almost linearly with the increase in actin concentration, both V_{max} and K_{app} values of L3 (-5) could not be determined.

Molecular Design for High Velocity. It was of our surprise that 2 of loop 2 mutants [L2 (-2) and L2 (C-1)] moved faster than the wild type (Table 4). Because we thought that *Chara* myosin has evolutionary established elaborated structure to move very fast, we expected that any manipulation of its amino acids sequence would perturb this structure and impair the velocity. Our results that even the fastest myosin could be made to move faster than the wild type suggested that we might be able to make various myosins move faster than their original by removing the positive charge from loop 2 and/or by adding positive charge to loop 3. To test this hypothesis, we manipulated loops 2 and 3 of *Dictyostelium* myosin. Loop 2 and loop 3 sequences of *Dictyostelium* myosin are as follows.

Loop 2 ^{612} FNDPNIAS*RAK*KGANFITVA ^{631}
Loop 3 ^{560} EPRF*S*K ^{565}.

We made 3 mutant myosins. S564K mutant myosin had one additional positive charge in loop 3 and R620A-K622A mutant myosin lost 2 positive charges from loop 2. S564K/R620A-K622A mutant myosin has these both of 2 mutations. Since actin-activated ATPase activity of these mutants and wild-type *Dictyostelium* myosin increased linearly with actin concentration due to low affinity for actin under our assay condition (34), we compared their ATPase activity at 95 μM (4 mg/ml) actin. Addition of one positive charge to loop 3 (S564K) enhanced the ATPase activity 1.7-fold higher than that of the wild type while leaving the velocity the same (Table 5, S564K). Removing 2 positive charges from loop 2 dramatically decreased the ATPase activity (Table 5, R620A-K622A). The R620A-K622A myosin could not translocate actin filaments probably due to low affinity for actin even in the presence of methylcellulose. While actin filaments attached to the R620A-K622A myosin-coated surface in the absence of ATP, the majority of the actin filaments dissociated on addition of ATP. Some stayed near the surface and exhibited random, lateral motion without making noticeable unidirectional axial movement. Adding one positive charge to loop 3 (S564K) in the R620A-K622A mutant myosin increased ATPase activity 3.8-fold higher than that of the R620A-K622A mutant and could move actin filaments (Table 5, S564K/R620A-K622A). The actin sliding velocity of the S564K/R620A-K622A myosin is 1.3-fold higher than that of wild type.

Discussion

Role of Loop 3 in the Actin Activation. Most myosins have positively charged a loop 2 with a cluster of lysine residues (Table 1). Many studies using various myosins suggested that the net charge of loop 2 controls the affinity of myosin for actin (25–29). Unlike other myosins, loop 2 of *Chara* myosin is very short and the

BIOCHEMISTRY

Table 4. Sequences, net charge, and activity of wild type and loop 2 mutants of *Chara* myosin motor domain

	Sequence*	Net charge	V_{max}† (Pi/head/s)	K_{app}† (μM)	Velocity‡ (μm/s)
L2 (−2)	FPADEG T*A* APS*A*FMSIG	−2	570	103	6.2 ± 0.3
L2 (C-1)	FPADEG T**K** APS*A*FMSIG	−1	690	69	5.9 ± 0.3
L2 (N-1)	FPADEG T*A* APS**K**FMSIG	−1	540	21	4.4 ± 0.3
WT	FPADEG T**K** APS**K**FMSIG	0	580	23	4.8 ± 0.2
L2 (N+0)	FPADEG*GGAAGG* T**K** APS**K**FMSIG	0	520	25	4.2 ± 0.2
L2 (N+2)	FPADEG*GGKKGG* T**K** APS**K**FMSIG	+2	630	8.2	2.4 ± 0.2
L2 (C+2)	FPADEG T**K**APS**K***KK*FMSIG	+2	500	8.3	1.7 ± 0.2
L2 (+4)	FPADEG*GGKKGG*T**K**APS**K***KK*FMSIG	+4	470	2.8	1.1 ± 0.1

*Positively charged amino acid and altered amino acid are shown in bold and italic, respectively.
†Values are averages of two measurements on two independent preparations.
‡Values are average ± SD of 40–50 actin filaments on two independent preparations.

number of positively charged amino acids in it is only 2, which are not in a cluster but separated (Table 1). In contrast, *Chara* myosin has much more positive net charge in loop 3 than any other myosins (Table 2). In agreement with this sequence feature, our results clearly showed a large contribution of loop 3 of *Chara* myosin to the V_{max} of the actin-activated ATPase activity (Fig. 2 and Table 3). In addition, the affinity of *Chara* myosin for actin was largely dependent on the positive charge of loop 3, which was shown by both the K_{app} of the actin-activated ATPase activity (Fig. 2 and Table 3) and actin-cosedimentation assays (see *Results*).

As mentioned earlier, the rate-limiting step of acto-*Chara* myosin ATPase is suggested to be the transition from a weekly bound state with actin to a strongly bound state with concomitant release of Pi (6). Because substitution of positively charged amino acids in loop 3 to alanine lowered V_{max}, the interaction with actin through loop 3 seems to play a critical role in triggering the transition from the weakly to the strongly bound state. Results using *Dictyostelium* mutant myosins also supported the relationship between loop 3 and actin-activated ATPase activity (Table 5). Combination of x-ray crystallographic results with information from electron microscopy revealed that loop 2 interacts with a subdomain 1 of actin molecule at which strong binding through hydrophobic interaction occurs and loop 3 interacts with a subdomain 1 of the next actin molecule (on the barbed-end side) in the same strand of double helical actin filament (35). This simultaneous interaction will make myosin head bind stably with 2 neighboring actin molecules in a filament. This interaction may, at the same time, alter the conformation of myosin the motor domain, which somehow deforms the active site and accelerates phosphate release. Variation in extent and manner of acto-myosin interactions would change the extent of the deformation of the active site. Among myosins so far measured, actin-activated ATPase activity of *Chara* myosin is the highest and this may be relevant to the fact that the net positive charge in loop 3 of *Chara* myosin is the largest among all myosins (Table 2).

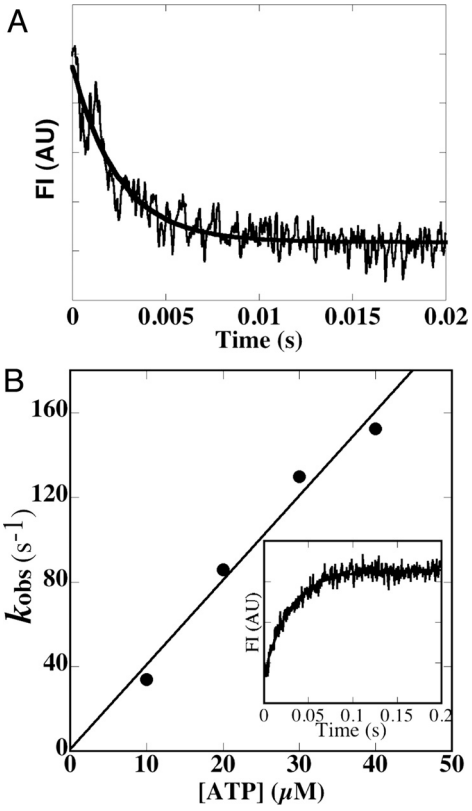

Fig. 3. Kinetic analysis of acto-L2 (+4). (*A*) MantADP dissociation from acto-L2 (+4). A solution containing 1 μM L2 (+4), 20 μM actin and 100 μM mantADP was mixed with 5 mM ATP (final concentration) at 25 °C. MantADP dissociation from acto-MD was monitored using fluorescence energy transfer between tryptophan of motor domain and mantADP. The transient is an average of 5 to 7 separate recordings and the solid line is a single exponential fit, which gave a rate constant (k_{-ADP}) of 406 s^{-1} in the example shown. Averaged value of 5 independent assays for 2 independent preparations was 480 ± 70 s^{-1} (n = 5). AU = arbitrary units. (*B*) ATP-induced dissociation of the pyrene-actin- L2 (+4) complex. Observed rate of ATP-induced dissociation (k_{obs}) at 25 °C was plotted against ATP concentrations (10 to 40 μM). Slope of the plot gave a value for K_1k_{+2} of 4.0 $\mu M^{-1}s^{-1}$. (*Inset*) Representative data when 0.5 μM pyrene-acto- L2 (+4) complex was mixed with 10 μM ATP (final concentration). Single exponential fit to the observed fluorescence change gave a rate constant of 34 s^{-1} (solid line).

Effect of Loop 2 Charge on the Velocity. When the net charge in loop 2 increased, K_{app} decreased (the apparent affinity for actin

Table 5. ATPase activity and velocity of WT and mutant *Dictyostelium* myosin II

	ATP ase activity* (Pi/head/s)	Velocity (μm/s)†
WT	1.4 ± 0.2	2.4 ± 0.2
S564K	2.4 ± 0.3	2.4 ± 0.2
R620A K622A	0.12 ± 0.01	0
S564K/R620A K622A	0.45 ± 0.06	3.1 ± 0.4‡

Actin-activated ATPase activity and velocity of wild type and mutant *Dictyostelium* myosins
*Values are averages ± SD of at least three measurements on two independent preparations. Each value was obtained by subtracted activities in the absence of actin from the measured values in the presence of 95 μM actin.
†Values are averages ± SD of 20–30 actin filaments on two independent preparations.
‡Velocity of S564K/R620A K622A myosin was done in the presence of 0.8% methylcellulose.

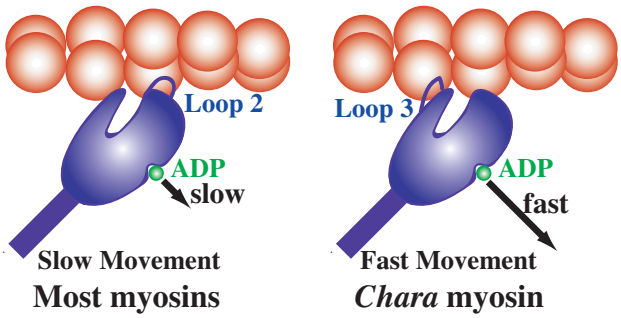

Fig. 4. Schematic diagram of strategy of *Chara* myosin for fast movement. For most myosins, the hydrophilic interaction with actin is mainly through loop 2, which slows ADP release and thus velocity (*Left*). In contrast for *Chara* myosin, hydrophilic interaction with actin is mainly through loop 3, which does not slow (*Right*).

increased) but V_{max} was less affected. In the loop 2 mutants, however, the velocity decreased with the decrease in K_{app} (Table 4). Decrease in the velocity was caused by the reduction in ADP dissociation rate from acto-*Chara* myosin motor domain (Fig. 3). Similar results for the effect of positive charge in loop 2 on the velocity were reported for smooth muscle myosin II (25). The inverse correlation between the net charge of loop 2 and the velocity may be a general rule for myosin velocity although an exceptional result was reported for slow myosin with very long loop 2. Addition of positive charges to loop 2 of myosin V did not alter the velocity (29). Since α-helix after loop 2 is connected to a β-strand that surrounds the nucleotide binding site of myosin (36), strong interaction with actin through loop 2 somehow reduces the ADP release rate and thus velocity. It surprised us that 2 of loop 2 mutants moved faster than wild type (Table 4).

Increase in the positive charge in both loop 2 and loop 3 lowered the K_{app} similarly, but their electrostatic interaction with actin affected the ATPase activity and the velocity differently. It is probably due to the difference in the stress exerted on the motor domain by their interaction with actin as mentioned above. The affinity for actin can be maintained by positive charge in either loop 2 or loop 3, but affinity increment through loop 2 accompanies reduction in the ADP release rate and thus lowers the velocity (Figs. 3 and 4). It is speculated that *Chara* myosin has evolved to keep the high affinity for actin through loop 3 and reduce the positive charge in loop 2 to enhance the ADP release rate for its high velocity.

Our results suggest that we can make various myosins move faster than the original one by reducing the positive charge from loop 2. To maintain actin affinity of the mutant myosin of which positive charge in loop 2 is decreased, the positive charge in loop 3 should be increased because charge alteration in loop 3 has little effect on velocity. This was also supported by the mutation experiments using *Dictyostelium* myosin (Table 5). Although the velocity of the *Dictyostelium* mutant myosin was far lower than that of *Chara* myosin, suggesting that there is intrinsic difference between *Dictyostelium* myosin and *Chara* myosin, the results obtained from different class myosin (class II) proved our hypothesis and supported our view that one of the reasons for the high velocity of *Chara* myosin is low positive charge in loop 2 and high positive charge in loop 3.

Materials and Methods

Protein Engineering, Expression, and Purification. A baculovirus transfer vector for *Chara* myosin motor domain (pFastBac MD) was made as mentioned previously (6). *Chara* myosin motor domain contains residues 4–746 of the *Chara* myosin heavy chain, a flexible linker (GGG), a Myc-epitope sequence (EQKLISEEDL), and a $(His)_8$-tag (Molecular weight: 86,676). A baculovirus transfer vector for *Chara* myosin motor domain with FLAG-tag (pFastBac MD with FLAG-tag) was generated as follows. pFastBac MD was cut with XhoI and SacI (a XhoI-SacI fragment of *Chara* myosin motor domain). pFastBac MD-Vneck (6) was cut with XhoI and SacI and legated with a XhoI-SacI fragment of pFastBac MD. The resultant protein, *Chara* myosin motor domain with FLAG-tag, encodes the N-terminal sequence (MSYYHHHHHHDYKDDDDK-NIPTTENLYFQGA) containing the sequence of $(His)_6$-tag and FLAG-tag (DYK-DDDDK), residues 4–746 of *Chara* myosin heavy chain, a flexible linker (GGG), a Myc-epitope sequence (EQKLISEEDL) and a $(His)_8$-tag (Molecular weight: 91,761). *Chara* myosin motor domains with FLAG-tag were L3 (-5), L3 (N-3), L3 (C-2), L2 (-2) and L2 (C-1). Mutations of loop 2, loop 3 of *Chara* motor domain and *Dictyostelium* myosins were made by site-directed mutagenesis using ExSite PCR-Based Site-Directed Mutagenesis Kit (Stratagene). Mutant and wild-type motor domains were expressed in insect cells and purified as mentioned previously (6). Mutant motor domains with FLAG-tag were purified as mentioned previously (6), except that Ni-affinity-purification was also done before FLAG-tag affinity purification. Wild-type and mutant *Dictyostelium* myosins were purified as described (37) and phosphorylated as described (38) using bacterially expressed myosin light chain kinase that carried a T166E mutation (39).

ATPase and in Vitro Velocity Assays. Steady-state ATPase activities were measured as described (5). The reactions were done in 25 mM KCl, 4 mM $MgCl_2$, 25 mM Hepes-KOH (pH 7.4), 1 mM ATP, 1 mM DTT, and 1 mg/ml BSA and at 30 °C, except for those in Fig. 1, which were done in 10 mM KCl, 4 mM $MgCl_2$, 20 mM Hepes-KOH (pH 7.4), 1 mM ATP, 1 mM DTT, and 1 mg/ml BSA and at 30 °C. The reactions were started by the addition of ATP, except for those of *Dictyostelium* full length myosin in Table 5, which were started by the addition of myosin as described (34). The velocity of MD was measured using an anti-myc antibody-based version of the in vitro actin filament gliding assay as described (6). The velocity of *Dictyostelium* myosin was measured as described (37). The velocity of actin filaments was measured in 25 mM KCl, 4 mM $MgCl_2$, 25 mM Hepes-KOH (pH 7.4), 3 mM ATP, 10 mM DTT and oxygen scavenger system (120 μg/ml glucose oxidase, 12.8 mM glucose, and 20 μg/ml catalase) at 25 °C. Methyl cellulose (0.8%) was added to the assay buffer to measure the velocity of L3(-4) and *Dictyostelium* myosin S564K/R620A-K622A.

Cosedimentation Assays. Cosedimentation assays were done as described (37). The solution used in the transient kinetic experiments was the same as that used in the steady-state ATPase measurements and in vitro velocity assays, except that nonhydrolyzable ATP analog AMP-PNP was used, instead of ATP.

Transient Kinetic Measurements. All kinetic experiments were done at 25 °C using an Applied Photophysics SX18MV stopped-flow spectrophotometer (dead time: 1.15 ms). The solution used in the transient kinetic experiments was the same as that used in the steady-state ATPase measurements and in vitro velocity assays. Dissociation of acto-motor domain by ATP was monitored through the change in fluorescence intensity of pyrene-labeled actin stabilized by phalloidin excited at 365 nm and detected after passing through a 389 nm cutoff filter. Dissociation of mantADP from acto-motor domain was monitored by the decrease in its fluorescence. MantADP were excited at 290 nm via fluorescence resonance energy transfer from tryptophan of motor domain and emission was observed after passing through a 389 nm cutoff filter.

ACKNOWLEDGMENTS. We thank Drs. Kazuo Sutoh and Takahide Kon of University of Tokyo, Tokyo, Japan, for allowing us to use a stopped-flow apparatus. This work was supported in part by Grants-in-Aid from the Ministry of Science, Culture and Education of Japan (to K. I.).

1. Kachar B, Reese TS (1988) The mechanism of cytoplasmic streaming in characean algal cells: Sliding of endoplasmic reticulum along actin filaments. *J Cell Biol* 106:1545–1552.
2. Yamamoto K, Kikuyama M, Sutoh-Yamamoto N, Kamitsubo E (1994) Purification of actin based motor protein from *Chara corallina*. *Proc Jpn Acad* 70:175–180.
3. Higashi-Fujime S, et al. (1995) The fastest actin-based motor protein from the green algae, *Chara*, and its distinct mode of interaction with actin *FEBS Lett* 375:151–154.
4. Kashiyama T, Kimura N, Mimura T, Yamamoto K (2000) Cloning and characterization of a myosin from characean alga, the fastest motor protein in the world. *J Biochem* 127:1065–1070.
5. Ito K, et al. (2003) Recombinant motor domain constructs of Chara corallina myosin display fast velocity and high ATPase activity. *Biochem Biophys Res Commun* 312:958–964.
6. Ito K, et al. (2007) Kinetic mechanism of the fastest motor protein, Chara myosin. *J Biol Chem* 282:19534–19545.

7. Kimura Y, Toyoshima N, Hirakawa N, Okamoto K, Ishijima A (2003) A kinetic mechanism for the fast movement of Chara myosin. *J Mol Biol* 328:939–950.
8. Onishi H, Mikhailenko SV, Morales MF (2006) Toward understanding actin activation of myosin ATPase: The role of myosin surface loops. *Proc Natl Acad Sci USA* 103:6136–6141.
9. Yamamoto K, Sekine T (1979) Interaction of myosin subfragment-1 with actin. I. Effects of actin binding on the susceptibility of subfragment-1 to trypsin. *J Biochem* 86:1855–1862.
10. Mornet D, Pantel P, Audemard E, Kassab R (1979) The limited tryptic cleavage of chymotryptic S-1: An approach to the characterization of the actin site in myosin heads. *Biochem Biophys Res Commun* 89:925–932.
11. Sutoh K (1982) An actin-binding site on the 20K fragment of myosin subfragment 1. *Biochemistry* 21:4800–4804.
12. Sutoh K (1982) Identification of myosin-binding sites on the actin sequence. *Biochemistry* 21:3654–3661.
13. Sutoh K (1983) Mapping of actin-binding sites on the heavy chain of myosin subfragment 1. *Biochemistry* 22:1579–1585.
14. Yamamoto K, Sekine T (1986) Difference between subfragment-1 and heavy meromyosin in their interaction with F-actin. *J Biochem* 99:199–206.
15. Chaussepied P (1989) Interaction between stretch of residues 633–642 (actin binding site) and nucleotide binding site on skeletal myosin subfragment 1 heavy chain. *Biochemistry* 28:9123–9128.
16. Mornet D, Ue K, Chaussepied P, Morales MF (1986) Modification of the actin interface of skeletal myosin subfragment-1 by treatment with dibromobimane. *Eur J Biochem* 159:555–561.
17. Yamamoto K (1989) Binding manner of actin to the lysine-rich sequence of myosin subfragment 1 in the presence and absence of ATP. *Biochemistry* 28:5573–5577.
18. Cheung P, Reisler E (1992) Synthetic peptide of the sequence 632–642 on myosin subfragment 1 inhibits actomyosin ATPase activity. *Biochem Biophys Res Comm* 189:1143–1149.
19. Bonafe N, Chaussepied P (1995) A single myosin head can be cross-linked to the N termini of two adjacent actin monomers. *Biophys J* 68(Suppl 4):35S–43S.
20. Andreev OA, Takashi R, Borejdo J (1995) Fluorescence polarization study of the rigor complexes formed at different degrees of saturation of actin filaments with myosin subfragment-1. *J Muscle Res Cell Motil* 16:353–367.
21. Andreev OA, Borejdo J (1997) Interaction of the heavy and light chains of cardiac myosin subfragment-1 with F-actin. *Circ Res* 81:688–693.
22. Spudich JA (1994) How molecular motors work. *Nature* 372:515–518.
23. Goodson HV, Warrick HM, Spudich JA (1999) Specialized conservation of surface loops of myosin: Evidence that loops are involved in determining functional characteristics. *J Mol Biol* 287:173–185.
24. Uyeda TQP, Ruppel KM, Spudich JA (1994) Enzymatic activities correlate with chimaeric substitutions at the actin-binding face of myosin. *Nature* 368:567–569.
25. Joel PB, Sweeney HL, Trybus KM (2003) Addition of lysines to the 50/20 kDa junction of myosin strengthens weak binding to actin without affecting the maximum ATPase activity. *Biochemistry* 42:9160–9166.
26. Furch M, Geeves MA, Manstein DJ (1998) Modulation of actin affinity and actomyosin adenosine triphosphatase by charge changes in the myosin motor domain. *Biochemistry* 37:6317–6326.
27. Knetsch ML, Uyeda TQ, Manstein DJ (1999) Disturbed communication between actin- and nucleotide-binding sites in a myosin II with truncated 50/20-kDa junction. *J Biol Chem* 274:20133–20138.
28. Yengo CM, Sweeney HL (2004) Functional role of loop 2 in myosin V. *Biochemistry* 43:2605–2612.
29. Hodges AR, Krementsova EB, Trybus KM (2007) Engineering the processive run length of Myosin V. *J Biol Chem* 282:27192–27197.
30. Uyeda TQ, Warrick HM, Kron SJ, Spudich JA (1991) Quantized velocities at low myosin densities in an in vitro velocity assay. *Nature* 352:307–311.
31. Joel PB, Trybus KM, Sweeney HL (2001) Two conserved lysines at the 50/20-kDa junction of myosin are necessary for triggering actin activation. *J Biol Chem* 276:2998–3003.
32. Millar NC, Geeves MA (1983) The limiting rate of the ATP-mediated dissociation of actin from rabbit skeletal muscle myosin subfragment 1. *FEBS Letters* 160:141–148.
33. Siemankowski RF, Wiseman MO, White HD (1985) ADP dissociation from actomyosin subfragment 1 is sufficiently slow to limit the unloaded shortening velocity in vertebrate muscle. *Proc Natl Acad Sci USA* 82:658–662.
34. Liu X, et al. (1998) Filament structure as an essential factor for regulation of Dictyostelium myosin by regulatory light chain phosphorylation. *Proc Natl Acad Sci USA* 95:14124–14129.
35. Rayment I, et al. (1993) Structure of the actin-myosin complex and its implications for muscle contraction. *Science* 261:58–65.
36. Rayment I, et al. (1993) Three-dimensional structure of myosin subfragment-1: A molecular motor. *Science* 261:50–58.
37. Ito K, Uyeda TQ, Suzuki Y, Sutoh K, Yamamoto K (2003) Requirement of domain–domain interaction for conformational change and functional ATP hydrolysis in myosin. *J Biol Chem* 278:31049–31057.
38. Ruppel KM, Uyeda TQ, Spudich JA (1994) Role of highly conserved lysine 130 of myosin motor domain. In vivo and in vitro characterization of site specifically mutated myosin. *J Biol Chem* 269:18773–18780.
39. Smith JL, Silveira LA, Spudich JA (1996) Myosin light chain kinase (MLCK) gene disruption in Dictyostelium: A role for MLCK-A in cytokinesis and evidence for multiple MLCKs. *Proc Natl Acad Sci USA* 93:12321–12326.